IOP Publishing European Journal of Physics
Eur. J. Phys. **41** (2020) 035401 (12pp) https://doi.org/10.1088/1361-6404/ab6501

From macro-measure of Franck–Hertz curves to micro-collisions between electrons and argon atoms

Li Huang[1], Hongfeng Lü[2], Weilong Liu[1], Li Xin[1], Haifa Zhao[1] and Yu Zhang[1]

[1] College of Physics, Harbin Institute of Technology, Harbin 150001, People's Republic of China
[2] College of Science, China Agricultural University, Beijing 100083, People's Republic of China

E-mail: lihuang2002@hit.edu.cn

Received 17 July 2019, revised 16 December 2019
Accepted for publication 23 December 2019
Published 24 February 2020

Abstract

A Franck–Hertz experiment is adopted in our undergraduate laboratory by using a cylindrical tetrode tube filled with argon vapor. The Franck–Hertz curves, i.e. the variation of the anode current via the accelerating voltage, are experimentally measured, and the key roles of the filament voltage, the control voltage, and the retarding voltage played in the experiments are studied. Diagrams of the micro-elastic/inelastic collisions between the electrons and argon atoms, which are of significance for students to build a connection between the macroscopic measurements and microscopic collisions occurring inside the Franck–Hertz tube, are schematically presented based on the experimental results. The peak/valley interval in the experimental Franck–Hertz curves of argon vapor increases as the accelerating voltage increases. The results further suggest that the lowest excitation energy of an argon atom cannot be exactly derived from the experimental results since all the four sub energy levels within the first excitation energy state of the argon atom are involved in the inelastic electron–atom collisions.

Keywords: Franck–Hertz curve, elastic collisions, inelastic collisions, lowest excitation energy

(Some figures may appear in colour only in the online journal)

1. Introduction

In 1914, James Franck (1882–1964) and Gustav Hertz (1887–1975) presented their experiments involving bombarding mercury vapor atoms with slow electrons, and discovered that the energy exchange between mercury atoms and the electrons occurred in distinct steps of 4.89 eV through electron–atom collisions [1]. They reported later that year on the light emission at $\lambda = 253.7$ nm by the mercury atoms that had absorbed energy from electron–atom collisions [2]. These so-called Franck–Hertz experiments were the first demonstration of the existence of the quantized atomic energy levels proposed by Bohr. Franck and Hertz were awarded the 1925 Nobel Prize in Physics for their 'discovery of the laws governing the impact of an electron upon an atom' [3].

The Franck–Hertz experiments laid the foundation of modern physics [4, 5], and are essential knowledge for students learning atomic physics and quantum mechanics. The reproduced experiment is universal in the undergraduate laboratory, and mostly carried out with mercury [6–9] and neon [10]. Argon is the third most abundant gas in the Earth's atmosphere, and the electron impact excitation of argon atoms is found in space applications [11, 12]. We reproduce the Franck–Hertz experiment on our undergraduate physics course with low-pressure argon vapor at room temperature, in which case the mean free path of the electrons remains almost unchanged, therefore the experimental results are stable. This enables students to carry out the experiments under various power supplies, to obtain an analyzable series of experimental data.

The main objective of this work is to help both students and tutors better understand the quantum concepts and phenomena from the Franck–Hertz experiments. By analyzing the macro-measured Franck–Hertz curves, we discuss the problems encountered by students but not shown in textbooks. Furthermore, the microscopic electron–atom collisions are graphically discussed, leading the students from macroscopic measurements to the microscopic electron–atom collisions. The discrete peaks and valleys in the experimental results indeed demonstrate the quantized energy in argon atoms. However, a certain low excitation energy of argon atoms cannot be derived from the data as assumed in the general experiments textbooks.

2. The argon Franck–Hertz tube

The setup we used for Franck–Hertz experiments in our undergraduate laboratory, including the Franck–Hertz tube, is bought from a Chinese company named Sichuan Shiji Zhongke Photoelectric Technology Co., Ltd. The tube is the most important component for the Franck–Hertz experiments. In analogy to the tube made for Franck–Hertz experiments with mercury [13, 14], we adopt an evacuated cylindrical shaped glass tube filled with low-pressure argon vapor at room temperature. The pressure inside the glass tube is difficult to measured and is estimated to be around a few mbar [12]. This tetrode tube, schematically shown in figure 1, is akin to an earlier described version [15].

In contrast to the plane-parallel electrode arrangement usually adopted in the undergraduate laboratory, our tube contains four cylindrical electrodes, i.e. the cathode K (dark grey) with the filament F (red) inside, the control grid G_1 (purple), the accelerating grid G_2 (blue), and the anode A (orange). The inner filament F is a two-way twisted tungsten wire coated with an alumina insulating layer. The cathode K is a ternary (Ba–Sr–Ca) oxide coated nickel pipe 1.2 mm in diameter. The work function of the cathode K should be as small as possible to guarantee the steady emission of electrons. The control grid G_1 and the

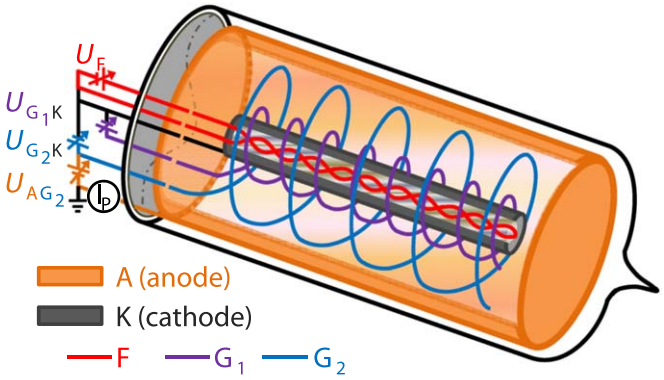

Figure 1. Schematic of the vacuum Franck–Hertz tube filled with argon vapor and its outside power supplies used in this experiment. The tube contains the filament F (red) and four cylindrical electrodes, i.e. the cathode K (dark grey), the control grid G_1 (purple), the accelerating grid G_2 (blue), and the anode A (orange).

accelerating grid G_2 are 1.8 and 11.8 mm wide helixes, which are rounded with molybdenum wires with 0.08 and 0.12 mm in diameter separately. The grid G_1 is located in close proximity to the cathode K, while the distance between K and G_2 is much longer to guarantee the collisions between the argon atoms and the moving electrons. The anode A, which is an aluminum-coated iron cylinder 16.0 mm in diameter, is located adjacent to the accelerating grid G_2 to collect the transmitted electrons. The length of all the above cylindrical electrodes is ∼28 mm.

The power supplies, i.e. the filament voltage U_F, the control voltage U_{G1K}, the accelerating voltage U_{G2K}, and the retarding voltage U_{AG2} of the tube are also schematically shown in figure 1. In the experiment, the filament under the heating voltage U_F (continuously variable from 0 to 5.0 V) indirectly heats the cathode K. The electrons, which are near the top of the Fermi distribution in the cathode K, penetrate the potential barrier and escape from the surface of the cathode K in a process called thermionic emission. The control voltage U_{G1K} (continuously variable from 0 to 3.0 V) is maintained at a small positive voltage to control the charge cloud formed by the emitted electrons over the surface of the cathode K. The emitted electrons are accelerated toward the anode passing through the accelerating electric field formed by the accelerating voltage U_{G2K} (continuously variable from 0 to 90.0 V). After moving through the accelerating grid G_2, the electrons are decelerated by the retarding voltage U_{AG2} (continuously variable from 0 to 10.0 V). Only when the kinetic energies carried by the electrons near G_2 exceed eU_{AG2} can they reach the anode A and give rise to the anode current I_p. The energies carried by the moving electrons depend on the collisions happened between the electrons and the argon atoms on the way. The magnitude of the anode current I_p is in order of 10^{-7} A and measured with a sensitive DC current amplifier as a function of the accelerating voltage U_{G2K}.

3. The first excitation energy state of argon atoms

Students need to know the first excitation energy state of an argon atom before the measurements. According to the NIST Atomic Spectra Database [16], there are four sub energy levels, $1s_2$, $1s_3$, $1s_4$, and $1s_5$, within the first excitation energy state of argon atoms.

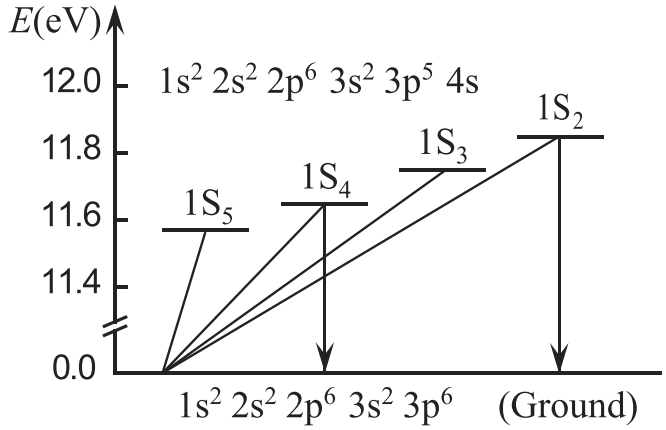

Figure 2. The first excitation energy level of an argon atom [16].

Figure 2 schematically shows these four sub energy levels of 11.83 eV, 11.72 eV, 11.62 eV, and 11.55 eV with respect to the ground energy state of 0 eV for the argon atom. An atom can be excited from a low-energy state to high-energy state in many ways, e.g. by absorbing certain energies carried by a specific photon. In Franck–Hertz experiments, an atom is excited to the first excitation energy state through inelastic collision, i.e. a moving electron with the kinetic energy equal to or larger than the first excitation energy of an atom collides with the atom and excites it to the first excitation state. Apart from inelastic collisions, elastic collisions might occur between an atom and a moving electron whose kinetic energy is lower than the first excitation energy of the atom in the Franck–Hertz tube. Based on the above knowledge, most students assume that the atom would be excited to the lowest sub energy level in the first excitation energy state. So it is worth mentioning that an argon atom can be theoretically be excited to each of the four sub energy levels shown in figure 2 through inelastic collision, which is not restricted by the selection rule of radiation jump. The probability for a specific argon atom being excited to which sub energy level depends on the velocity distribution of the moving electrons and the excitation cross section of each sub energy level [17].

However, all the excited atoms undergo de-excitation following the selection rule no matter which way they are excited. The de-excitation of a meta-stable atom from the sub energy levels $1s_3$ and $1s_5$ with a lifetime in order of $\sim 10^{-3}$ s is forbidden by the selection rule, whereas the sub energy levels $1s_2$ and $1s_4$ de-excite within a lifetime in the order of $\sim 10^{-8}$ s [17]. Take one of the four sub energy levels in the first excitation energy state of argon atoms, for example the sub energy level $1s_2$ of 11.83 eV. The corresponding wavelength of the emitted photons can be calculated with the Planck relation:

$$\lambda = \frac{hc}{\Delta E_0} = \frac{6.63 \times 10^{-34} \times 3.00 \times 10^{8}}{1.60 \times 10^{-19} \times 11.83} = 1.051 \times 10^{2}\,(\text{nm}).$$

We cannot observe directly such emission in Franck–Hertz experiments since it is the deep ultraviolet light outside the visible region. However, students are advised to infer and picture the micro-collision processes occurring in the tube through analyzing the experimentally measured Franck–Hertz curves. In this way, we help students to build a bridge connecting the macro-measure of the Franck–Hertz curve and micro-elastic/inelastic electron–atom collisions occurring inside the Franck–Hertz tube.

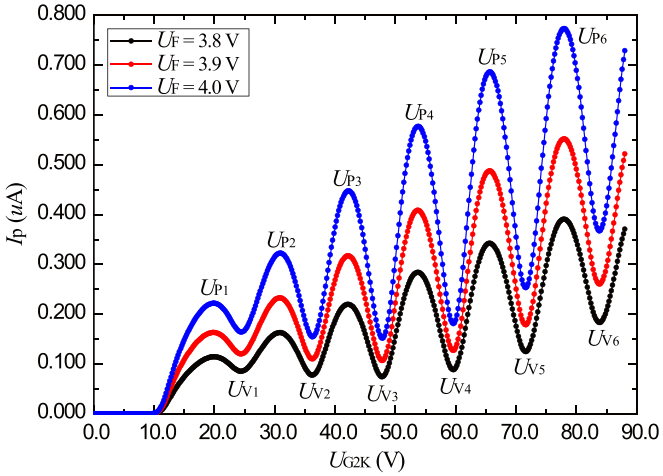

Figure 3. Experimentally measured Franck–Hertz curves with filament heating voltage U_F of 3.8 V (black), 3.9 V (red), and 4.0 V (blue). Correspondingly, the control voltage U_{G1K} is fixed as 1.0 V and the retarding voltage U_{AG2} as 8.0 V. The U_{G2K} values corresponding to each peak and valley of the curve are denoted as U_{Pi} and U_{Vi} (i = 1, 2, 3, 4, 5, 6), respectively.

4. Role of power supplies on macro-measured Franck–Hertz curves

In order to enlighten students on the underlying physics of the Franck–Hertz experiment, they are advised to carry out the macro-measure of the anode current I_p variations with various power supplies of U_F, U_{G1K}, and U_{AG2}, under the accelerating voltage U_{G2K} increasing from 0 to 88.0 V with a step of 0.2 V.

4.1. Role of the filament heating voltage U_F

First, the students measure the Franck–Hertz curves at various U_F between 3.8 and 4.0 V, to discover the role the filament heating voltage U_F plays in the experiments. Under each value of U_F, the control voltage U_{G1K} and the retarding voltage U_{AG2} are fixed as 1.0 V and 8.0 V, respectively. The experimentally measured Franck–Hertz curves with the filament heating voltage U_F of 3.8 V (black), 3.9 V (red), and 4.0 V (blue) are shown in figure 3.

Slightly increasing the filament heating voltage U_F results in an overall significant increase of the anode current I_p, which means that more moving electrons overcome the retarding electric field and contribute to the anode current I_p under the same accelerating voltage U_{G2K}. This is due to the temperature of the cathode K increasing dramatically with a small increment of the filament heating voltage U_F, and the quantities of the electrons emitted from the cathode K by thermionic emission increase sharply according to the Richardson–Dushman equation [18]

$$J_e = A_e T_e^2 \exp(-W_e/kT_e)$$

where J_e is the current density formed by the emitted electrons, A_e is the Richardson's constant of the cathode K, T_e is the absolute temperature of the cathode K, W_e is the thermionic work function of the cathode K, and k is Boltzmann constant.

As shown in figure 3, the anode current I_p rises from zero at ~9.8 V for the three curves. This value is mainly determined by the retarding voltage U_{AG2} (fixed as 8.0 V), the control

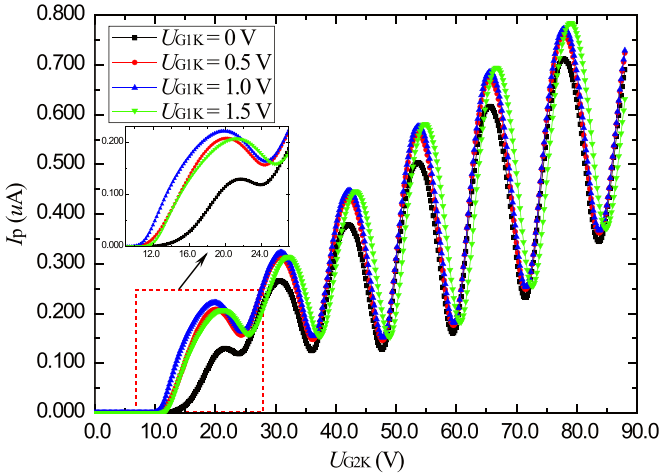

Figure 4. Experimentally measured Franck–Hertz curves with the control voltage U_{G1K} of 0 V (black), 0.5 V (red), 1.0 V (blue), and 1.5 V (cyan). Correspondingly, the filament heating voltage U_F is fixed as 4.0 V and the retarding voltage U_{AG2} as 8.0 V.

voltage U_{G1K} (fixed as 1.0 V), and the contact potentials between the electrodes. Each metal has its unique work function W_e, so there is contact potential between any two of the four electrodes, i.e. the cathode K, the control grid G_1, the accelerating grid G_2, and the anode A. It is hard to experimentally measure the contact potential inside the Franck–Hertz tube. However, the experimental results indicate that the contact potential is small with the same sign as the retarding voltage U_{AG2}, and it also hinders the moving electrons from reaching the anode.

The experimental results shown in figure 3 imply that the anode current I_p is hard to measure accurately if the filament heating voltage U_F is below 3.8 V. On the other hand, the anode current I_p might overflow and the filament ages rapidly when the filament heating voltage U_F is above 4.0 V. Therefore, the optimized U_F is 4.0 V for this tube in the following experiments. Additionally, the positions of the peaks and valleys, denoted as U_{Pi} and U_{Vi} in figure 3, do not shift with an increase in the filament heating voltage. This suggests that the number of emitted electrons, which is determined mainly by the filament heating voltage U_F, has no influence on the micro-collisions between the moving electrons and the argon atoms.

4.2. Role of control voltage U_{G1K}

Second, students measure the Franck–Hertz curves at various U_{G1K} between 0 and 1.5 V to study the role of the control voltage U_{G1K} played in the Franck–Hertz experiment. Under each value of U_{G1K}, the filament heating voltage U_F and the retarding voltage U_{AG2} are separately fixed as 4.0 V and 8.0 V. The experimentally measured Franck–Hertz curves with the control voltage U_{G1K} of 0 V (black), 0.5 V (red), 1.0 V (blue), and 1.5 V (cyan) are shown in figure 4.

The experimentally measured Franck–Hertz curves in figure 4 show that increasing the control voltage U_{G1K} results in an overall increase of the anode current I_p with a negligible shift. The inset of figure 4 shows a significant increase of the first peak anode current which is unobvious when U_{G1K} is zero. The kinetic energies of the electrons very recently escaped from the cathode surface are very low and the energy distribution is close to the Boltzmann distribution, with a mean energy near kT_e with thermionic emission. The emitted electrons form an electron cloud over the surface of the cathode K and hinder the successive emission

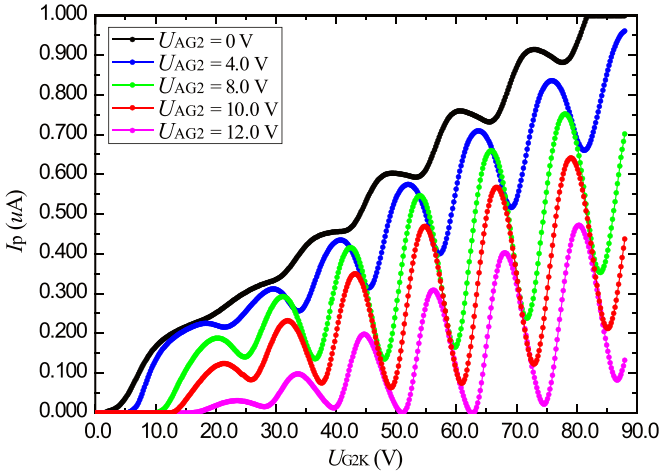

Figure 5. Experimentally measured Franck–Hertz curves with the retarding voltage U_{AG2} of 0 V (black), 4.0 V (blue), 8.0 V (cyan), 10.0 V (red), and 12.0 V (violet). Correspondingly, the filament heating voltage U_F is fixed as 4.0 V and the control voltage U_{G1K} as 1.0 V.

of the other electrons when the control voltage is zero. With a small positive control voltage U_{G1K}, more emitted electrons move forwards to the grid G_1 attributed to the Schottky effect, and the energy density of the electron cloud over the surface of the cathode K is remarkably averaged. The electric field E_{G1K} between K and G_1, which are coaxial cylinders, is described by the following equation, considering the length of the cylinders is much larger than the diameters [19]:

$$E_{G1K} = \frac{U_{G1K} - U_{con.}}{r_K \ln \frac{r_{G1}}{r_K}}.$$

Here $U_{con.}$ is the contact potential between K and G_1, r_K is the diameter of K, and r_{G1} is the diameter of G_1.

In our Franck–Hertz tube, described earlier, r_K is comparable with r_{G1} whereas the diameter of G_2 is much bigger than r_K, so the electric field E_{G1K} formed by U_{G1K} is much stronger than the electric field E_{G2K} formed by U_{G2K} when U_{G2K} is below U_{P1}. This contributes to the noticeable increase of the first peak and its shift to lower U_{G2K}, whereas all the following peaks of the anode current I_p have almost the same increment as the accelerating voltage U_{G2K} increases. From the experimental results shown in figure 4, students optimize the control voltage as 1.0 V for the tube in the following experiments.

4.3. Role of retarding voltage U_{AG2}

The last in the series of experiments for the students is to study the role played by the retarding voltage U_{AG2}. With the optimized U_F and U_{G1K} as 4.0 V and 1.0 V, students measure the Franck–Hertz curves at various U_{AG2} from 0 V to 12.0 V. The experimentally measured Franck–Hertz curves with the retarding voltage U_{AG2} of 0 V (black), 4.0 V (blue), 8.0 V (cyan), 10.0 V (red), and 12.0 (violet) are shown in figure 5.

The Franck–Hertz curve without the retarding voltage (see the black curve in figure 5) only has unobvious peaks and valleys under higher accelerating voltage U_{G2K}. Increasing the

retarding voltage U_{AG2} results in the distinction between the peaks and valleys becoming more obvious, as well as an overall decrease of the anode current I_p. The electrons need greater energy to overcome the retarding electric field as the retarding voltage U_{AG2} increases, so less moving electrons overcome the retarding electric field under the same accelerating voltage U_{G2K} by the rule of probability and statistics. Meanwhile, increasing the retarding voltage U_{AG2} results in the positions of the extremes shifting to higher U_{G2K}.

As can be seen from figure 5, the first peak and valley in the black curve are off when the retarding voltage U_{AG2} is off. From the previous analysis of figure 3, we know the position of the first peak U_{P1} should be larger than the first excitation voltage U_0 (theoretically from 11.55 V to 11.83 V for argon atoms, as shown in figure 2) since the anode current I_p rises from zero at a certain accelerating voltage U_{G2K}. When the accelerating voltage U_{G2K} is around 11.55 V and the retarding voltage U_{AG2} is zero, the accelerated electron would reach the anode A even if it only experienced one inelastic electron–atom collision. Therefore, almost all the accelerated electrons contribute to the anode current and no first peak/valley is observed in the black curve. In contrast, the retarding field is difficult for the accelerated electrons to cross when the retarding voltage U_{AG2} is very large, i.e. 12.0 V. The position of the first peak U_{P1} is 23.6 V and the corresponding anode current is very low in the violet curve. From the experimental results shown in figure 5, students would optimize the retarding voltage U_{AG2} as 8.0 V.

5. Results and discussions

After carrying out measurements of the Franck–Hertz curves systematically, students find out that no matter how the Franck–Hertz curves (particularly the first peak/valley) vary with the outside potentials, the peaks/valleys in the curves are always discrete and the peak/valley intervals seem to be equidistant. Students then strive to explain the macroscopic phenomena observed, and are encouraged to discuss and debate on the following subjects according to their experimental results.

5.1. Micro-collisions occurring in the tube

Based on the macroscopic variations of the anode current I_p measured in the Franck–Hertz curve, students are advised to infer the microscopic processes between the moving electrons and argon atoms which occurred in the Franck–Hertz tube. Figure 6 shows the sketches of the elastic collisions (a) and the inelastic collisions (b) between the moving electrons and the argon atoms in the sectional view of the tube. As we know, the higher the accelerating voltage U_{G2K}, the more the gained energies of the moving electrons. The color from green to red of the moving electrons (the small circles) in figure 6 represents the energy they gained from low to high under various accelerating voltages U_{G2K}.

In figure 6(a), the electrons with low kinetic energies (the inner green circles) emitted from the surface of the cathode K (the middle black dot) are transmitted through the control grid G_1 (the purple dashed line) towards the accelerating grid G_2 (the blue dashed line) under the accelerating voltage U_{G2K}. If the energies of most electrons (the small circles in red in figure 6(b)) around the accelerating grid G_2 are above eU_{AG2}, they can reach the anode A (the orange solid line) and the anode current I_p increases; otherwise the electrons (the small circles in green figure 6(a)) have to stay around the accelerating grid G_2 and the anode current I_p goes down.

We know that the experimentally measured anode current I_p gradually increases to the first peak from zero when we slowly increase the accelerating voltage U_{G2K} from 0 to U_{P1}. The

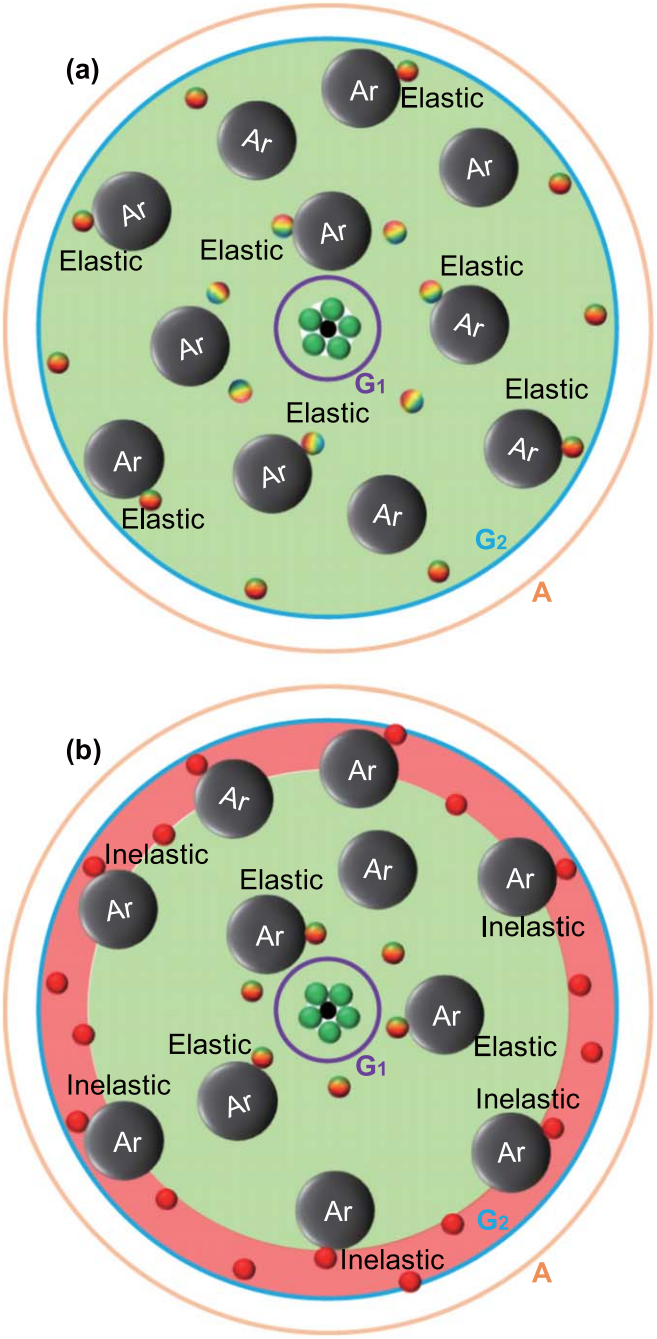

Figure 6. Sketches of the elastic collisions (a) and the inelastic collisions (b) between moving electrons and argon atoms in the sectional view of the tube. Small circles in colors from green to red represent the electrons with the kinetic energy from low to high. The big black circles represent the argon atoms. The inner black dot represents the cathode K. The purple and blue dashed lines represent the grid G_1 and G_2 respectively; the outer orange line represents the anode A.

macroscopic rising stage of the Franck–Hertz curve corresponds to the microscopic elastic collisions between the electrons and argon atoms. The kinetic energy of a moving electron gained from the accelerating electric field is below eU_{P1} and not high enough to excite an argon atom (the big black circles) under such circumstances, therefore the moving electrons only experience elastic collisions when they collide with argon atoms. The whole accelerating electric field is an elastic collision zone (the green area), as shown in figure 6(a). The moving electrons lose negligible energy during each elastic collision, since the electrons are over one thousand times less than even the lightest atoms, which means more and more moving electrons can overcome the retarding electric field and contribute to the anode current I_p.

The experimentally measured anode current I_p gradually decreases to the first valley from the first peak when we continuously increase the accelerating voltage U_{G2K} from U_{P1} to U_{V1}. The macroscopic falling stage of the Franck–Hertz curve corresponds to the microscopic inelastic collisions between the electrons and argon atoms. Once the accelerating voltage U_{G2K} reaches U_{P1}, a moving electron might gain enough kinetic energy near the grid G_2, and might impart its certain energy to an argon atom exciting it to the first excitation energy state through inelastic collisions. With U_{G2K} increasing from U_{P1} to U_{V1}, more moving electrons might excite argon atoms and an inelastic collision zone (the red area), as shown in figure 6(b), appears. The electrons which only experienced inelastic collision around the accelerating grid G_2 are not able to overcome the retarding electric field with their left energies, therefore less electrons reach the anode and the anode current I_p starts to fall.

As the accelerating voltage U_{G2K} continues to increase, the electrons which have experienced inelastic collision with argon atoms continue to gain kinetic energies, and the inelastic collision may happen periodically. The microscopic processes as described above happen repeatedly, and so the experimentally measured Franck–Hertz curve is an analogy to a periodic recurrent oscillation of the anode current I_p.

5.2. Peak/valley intervals in Franck–Hertz curves

The periodic structure of the measured Franck–Hertz curve indeed experimentally confirms the quantized, discrete energy levels in the Bohr model of the atom. However, can the first excitation energy level be derived from the peak/valley intervals, as generally assumed in the physics experiments textbooks? In order to answer this question, students are advised to study the positions of the extremes and peak/valley intervals in the Franck–Hertz curve experimentally measured with optimized U_F, U_{G1K}, and U_{AG2}, which are respectively set as 4.0 V, 1.0 V, and 8.0 V. To obtain more extremes, we sweep the accelerating voltage from 0 to 100.0 V with a step of 0.2 V. The positions of the first peak and valley, which vary irregularly with U_{G1K} and U_{AG2} as discussed in the section above, are not taken into account in the following discussion.

Table 1 lists the positions, i.e. the accelerating voltage U_{Pi} and U_{Vi} ($i = 1, 2, 3, 4, 5, 6$), corresponding to the peaks and the valleys, and their intervals ΔU_{Pi} and ΔU_{Vi}, i.e. the accelerating voltage intervals between adjacent peaks/valleys in the above optimized Franck–Hertz curve. The experimentally derived peak/valley intervals $\Delta U_{Pi}/\Delta U_{Vi}$ in table 1 show neither is equidistant, and the higher the accelerating voltage U_{G2K}, the larger the spacing of ΔU_{Pi} and ΔU_{Vi}. This regular pattern of the peak/valley intervals is true for all the experimentally optimized Franck–Hertz curves in our class, and it is also valid in the experiments with mercury and neon atoms [9].

We attribute the slight increment of peak/valley intervals to the elastic/inelastic electron–atom collisions which might occur in the experiments. Although the electrons lose negligible energy by elastic collisions with argon atoms, the directions of the electron

Table 1. Positions of extremes and peak/valley intervals of the Franck–Hertz curve experimentally measured with U_{F}, U_{G1K}, and U_{AG2} of 4.0 V, 1.0 V, and 8.0 V.

i	1	2	3	4	5	6	7
$U_{\mathrm{P}i}$	19.9	30.8	42.2	53.8	65.6	78.0	90.6
$U_{\mathrm{V}i}$	24.2	36.2	47.8	59.6	71.6	83.8	96.4
$\Delta U_{\mathrm{P}i} = U_{\mathrm{P}i}$-$U_{\mathrm{P}i\text{-}1}$	None	10.9	11.4	11.6	11.8	12.4	12.6
$\Delta U_{\mathrm{V}i} = U_{\mathrm{V}i}$-$U_{\mathrm{V}i\text{-}1}$	None	12.0	11.6	11.8	12.0	12.2	12.6

velocities are changed randomly. So the electron energy distribution is broad and nearly isotropic in velocity space after many elastic collisions [20]. Each of the four sub energy levels in the first excitation energy state of the argon atom might be excited through inelastic collisions regardless of the selection rule, as we mentioned earlier. Therefore the peaks of the Franck–Hertz curve relate all the four sub energy levels within the first excitation energy state of argon atoms. Within a very short time in the order of 10^{-8} s after being excited, the atoms in the excited states of $1s_2$ and $1s_4$ undergo de-excitation to the ground state. These atoms might collide with the moving electrons and be excited one further time. This implies that the number of the excited atoms in these two excited energy states is dramatically changed due to the inelastic collisions and the de-excitation, whereas the number of the atoms in the meta-stable energy states of $1s_3$ and $1s_5$ almost remains stable, since the meta-stable atoms have a lifetime in the order of 10^{-3} s. Therefore the valleys of the Franck–Hertz curve mainly relate to the two sub energy levels of $1s_2$ and $1s_4$ within the first excitation energy state of argon atoms. Furthermore, the energy level of $1s_2$ contributes more to the valleys since its excitation cross section is about three times greater than that of the $1s_4$ energy level [11].

On the other hand, the energy transfer efficiency during inelastic collisions cannot always be one hundred percent. The electrons which have experienced inelastic collisions have certain energies left and the accumulated electrons energies increase as the accelerating voltage increases.

6. Conclusions

The typical Franck–Hertz experiment is reproduced with low-pressure argon vapor at room temperature in our undergraduate laboratory. In order to help both students and tutors better understand the quantum concepts and phenomena from Franck–Hertz experiments, the influences of three power supplies of the Franck–Hertz tube, i.e. the filament voltage U_{F}, the control voltage U_{G1K}, and the retarding voltage U_{AG2} on the experimentally measured Franck–Hertz curves are studied. The microscopic elastic/inelastic electron–atom collisions are schematically presented, leading students from macroscopic measurements to microscopic electron–atom collisions. The experimental results show that both the peak interval $\Delta U_{\mathrm{P}i}$ and the valley interval $\Delta U_{\mathrm{V}i}$ become larger with increasing accelerating voltage. Although the experimentally measured $\Delta U_{\mathrm{P}i}$ and $\Delta U_{\mathrm{V}i}$ are close to the four sub energy levels in the first excitation energy state of argon atoms, the first excitation energy level of an argon atom is difficult to determine exactly, because all the four sub energy levels are involved in the inelastic electron–atom collisions occurring in Franck–Hertz experiments.

Acknowledgments

L Huang, W Liu, L Xin, H Zhao, and Y Zhang appreciate the support from the Research Project on the Top-notch Scientific Students Training, Department of Higher Education, Ministry of Education, P R China (Grant No. 20180215), Research Project on Teaching Reform of Higher Education, Heilongjiang Province, P R China (Grant No. SJGY20170642).

ORCID iDs

Li Huang https://orcid.org/0000-0002-1584-9053

References

[1] Franck J and Hertz G 1914 Über Zusammenstösse zwischen Elektronen und den Molekülen des Quecksilberdampfes und die Ionisierungsspannung desselben *Verh. Deut. Phys. Ges.* **16** 457
[2] Franck J and Hertz G 1914 Über die Erregung der Quecksilberresonanzlinie 253.6 $\mu\mu$ durch Elektronenstösse *Verh. D. Phys. Ges.* **16** 512
[3] The Nobel Prize 2020 The Nobel Prize in Physics 1925 (https://nobelprize.org/nobel_prize/physics/laureates/1925/)
[4] Gearhart C A 2014 The Franck-Hertz experiments, 1911–1914 experimentalists in search of a theory *Phys. Perspect.* **16** 293
[5] Robson R E, White1 R D and Hildebrandt M 2014 One hundred years of the Franck-Hertz experiment *Eur. Phys. J.* D **68** 188
[6] Genolio R J 1973 Average energy of electrons in a Franck-Hertz tube *Am. J. Phys.* **41** 288
[7] McMahon D R A 1983 Elastic electron-atom collision effects in the Franck-Hertz experiment *Am. J. Phys.* **51** 1086
[8] Sigeneger F, Winkler R and Robson R E 2003 What really happens with the electron gas in the famous Franck-Hertz experiment? *Contrib. Plasma Phys.* **43** 178
[9] Rapior G, Sengstock K and Baev V 2006 New features of the Franck-Hertz experiment *Am. J. Phys.* **74** 423
[10] Kash M M and Shields G C 1994 Using the Franck-Hertz experiment to illustrate quantization *J. Chem. Educ.* **71** 466
[11] Ajellot J M, James G K, Franklin B and Howell S 1990 Study of electron impact excitation of argon in the extreme ultraviolet: emission cross section of resonance lines of Ar I, Ar II *J. Phys. B: At. Mol. Opt. Phys.* **23** 4355
[12] Magyar P, Korolov I and Donkó Z 2012 Photoelectric Franck-Hertz experiment and its kinetic analysis by Monte Carlo simulation *Phys. Rev.* E **85** 056409
[13] Rosenfeld J H and Tyler C 1965 Homemade Franck-Hertz tube *Am. J. Phys.* **33** 849
[14] Tyler C E 1967 Simplified homemade Franck-Hertz tube *Am. J. Phys.* **35** 541
[15] Liu F H 1987 Franck-Hertz experiment with higher excitation level measurements *Am. J. Phys.* **55** 366
[16] Hayashi M 2003 NIFS-DATA-72 (http://www.nifs.ac.jp/report/NIFS-DATA-072.pdf)
[17] Scott Schappe R, Bruce Schulman M, Anderson L W and Lin C C 1994 Measurements of cross sections for electron-impact excitation into the metastable levels of argon and number densities of metastable argon atoms *Phys. Rev.* A **50** 444
[18] Kun H 1966 *Solid State Phys.* 1st edn (Beijing: People's Education Press) pp 286–7
[19] Yan Y M and Wang K X 1995 *Modern Physics Experiments* 2nd edn (Changchun: Jilin University Press) pp 44–8
[20] Robson R E, Li B and White R D 2000 Spatially periodic structures in electron swarms and the Franck-Hertz experiment *J. Phys.* B **33** 507